

THREE-DIMENSIONAL MODELING AND VISUALIZATION OF WHOLE NORWAY SPRUCE LATEWOOD TRACHEIDS

Stig L. Bardage

Research Scientist
Wood Ultrastructure Research Center
Swedish University of Agricultural Science
Department of Wood Science
P.O. Box 7008
SE-750 07 Uppsala, Sweden

(Received September 2000)

ABSTRACT

The three-dimensional morphology of four whole Norway spruce latewood tracheids is described in this work. Tracheids are shown to have a characteristic shape composed of five different morphological zones. Visualization of the different morphological zones was accomplished with the use of computerized three-dimensional (3D) reconstruction. 3D reconstructions were generated from stacks of micrographs obtained from serial sections of a wood block. The micrographs were processed and integrated in a CAD-based computerized modeling system using Non-Uniform Rational B-Splines (NURBS), which produces 3D reconstructions consisting of surfaces or volumetric bodies. Volumetric changes in relation to hydration state of latewood tracheid segments were studied. It was found that tracheid tips swell less than central regions, and that as a consequence of swelling, the cell walls of Norway spruce latewood tracheids expand inward towards the lumen.

Keywords: Three-dimensional, reconstruction, modeling, spruce, *Picea abies*, latewood tracheids, tracheid width, cell-wall thickness, swelling, shrinkage.

INTRODUCTION

Tracheid distribution, length, width, and cell-wall thickness of a variety of tree species have been continuously studied by many scientists (Helander 1933; Vasiljevic 1955; Bannan 1965; Fengel 1969; Panshin and de Zeeuw 1980; Atmer and Thörnqvist 1982; Saränpää 1994; Tyrväinen 1995; Lindström 1997; Herman et al. 1998). These types of data were often derived from measurements performed on sections or macerated tissue. These measurements often show great variations and normally do not take into account longitudinal variations of tracheids or their three-dimensionality. The microstructure of tracheids is known to be important for the physical and mechanical properties of wood and wood products. It will also influence the physical and mechanical properties of pulp and paper.

Only a few attempts to produce three-dimensional (3D) reconstructions of wood structure at the microscopical level have been made

so far (Lewis 1935; Suzuki et al. 1991; Fujii 1993; Fujita and Saiki 1996; Wang and Shaler 1998). In early work by Lewis (1935), serial transverse sections were used to study the arrangement and shape of pine tracheids. 3D visualization was achieved with the use of wax plate reconstructions. Suzuki et al. (1991) visualized the arrangement of wood cells in poplar by connecting their centers of gravity along a stack of images. Fujii (1993) studied the anatomy of some Japanese species of *Fragaceae* on resin casts with scanning electron microscopy. The resin casts were achieved by embedding dry wood blocks in polystyrene and completely removing cell walls through repeated treatments with peroxide/acetic acid solutions and sulfuric acid. Fujita and Saiki (1996) created a 3D reconstruction of the distribution of vessels in *Aesculus turbinata*. In a more technical oriented paper, Wang and Shaler (1998) presented computer simulations of the three-dimensional microstructure of wood fiber composite materials, although in this

study fibers were represented as rigid cylinders. 3D models are now being used more frequently in biological science to provide new perspectives into the morphological organization of biological structures and tissues (Emons and Mulder 1998; Zelling and Perktold 1998).

Wood shrinks anisotropically during drying. In coniferous wood, this phenomenon has been considered to arise mainly from the difference in shrinkage between earlywood and latewood, although it is influenced by ray tissue, microfibrillar orientation, and pit structure (Kollmann and Côté 1984). However, separated earlywood by itself has been reported to show transverse anisotropic shrinkage (Pentoney 1953; Nakato and Kajita 1955; Watanabe et al. 1998). This fact suggests that anisotropic shrinkage may also be related to cell shape and arrangement.

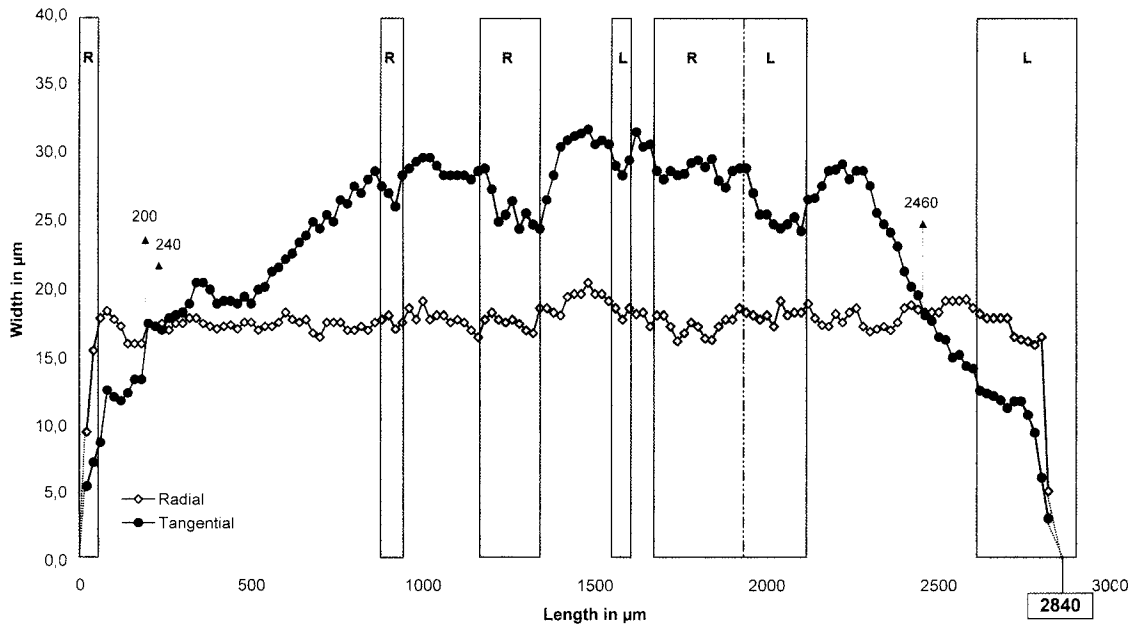
A methodology for computerized 3D reconstruction and visualization of wood microstructure has been developed within the Wood Ultrastructure Research Centre (WURC), Department of Wood Science, Swedish University of Agricultural Sciences, Uppsala, Sweden. 3D reconstructions are easily generated from stacks of micrographs obtained from serial sections of wood blocks. The micrographs are processed and integrated in a CAD-based computerized modeling system using Non-Uniform Rational B-Splines (NURBS) for the extraction of shapes. 3D reconstructions consisting of surfaces or volumetric bodies can be produced. The 3D models can be moved in X, Y, and Z directions allowing tilt and rotation. This allows the examination of reconstructions from different angles. Reconstructions can also be digitally sectioned and deformed and are capable of providing linear and volumetric measurement data. Norway spruce wood and pulp fibers are currently being studied using this technique. Image analysis and computerized 3D reconstruction were combined in the present work to reveal the micromorphology of whole Norway spruce latewood tracheids as a first step in the modeling of whole tracheid structure.

The objective of the present work was to study whole tracheid morphology and physical behavior in wood with the aid of computerized 3D reconstruction. This type of approach may provide a more detailed understanding of Norway spruce (*Picea abies*) wood fiber structure and properties.

MATERIALS AND METHODS

The samples used in this work came from a wood disc of Norway spruce (*Picea abies* [L.] Karst) collected at one quarter of tree stem height from a tree that was growing in the center of Sweden (Ludvika/Hällefors). The tree was 51 years old and the stem was growing with an inclination of 10°. A block (10 mm × 10 mm × 15 mm) comprising year rings 38–43 was taken from the outer part of the disc in an area free from compression wood and was prepared for serial sectioning using a sledge microtome. A total of 192 consecutive transverse sections (20 μ thick) were made without further pretreatment. The shortest unit length corresponds to 20 μm. Sections were mounted on objective glasses with water and scanned for tracheid tips with a light microscope to allow localization of a suitable area to begin image acquisition. One hundred forty-two transverse sections covered four whole tracheids belonging to one and the same radial row. Sequential images of hydrated transverse sections were acquired using a light microscope fitted with a CCD-camera attached to a computer (Pentium II). The sections were then dried at room temperature and coated with carbon prior to observations with a scanning electron microscope (JEOL JSM-5800LV). Sequential images of dried sections were taken with the scanning electron microscope (SEM) at the same position as for the hydrated samples. All images were stored and processed digitally. The four latewood tracheids studied, which derived from the same cambium mother cells, were numbered in a decreasing sequence (9, 8, 7, and 6) towards the year ring border at the latewood side. Image analysis was performed with the softwares ImagePro PLUS

Dimensional variation along the length of tracheid 6



FIGS. 1–4. Variation in radial and tangential widths along the length of dried latewood tracheids. Shaded areas represent neighboring rays. R (right) and L (left) denote the position of rays seen from a tangential view.

Dimensional variation along the length of tracheid 7

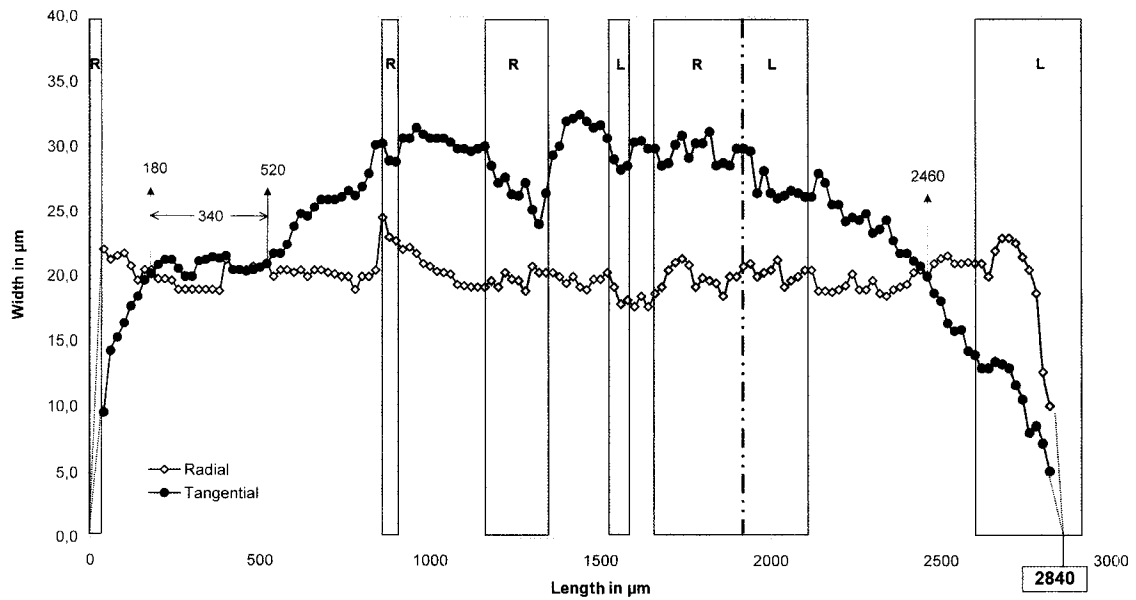


FIG. 2.

Dimensional variation along the length of tracheid 8

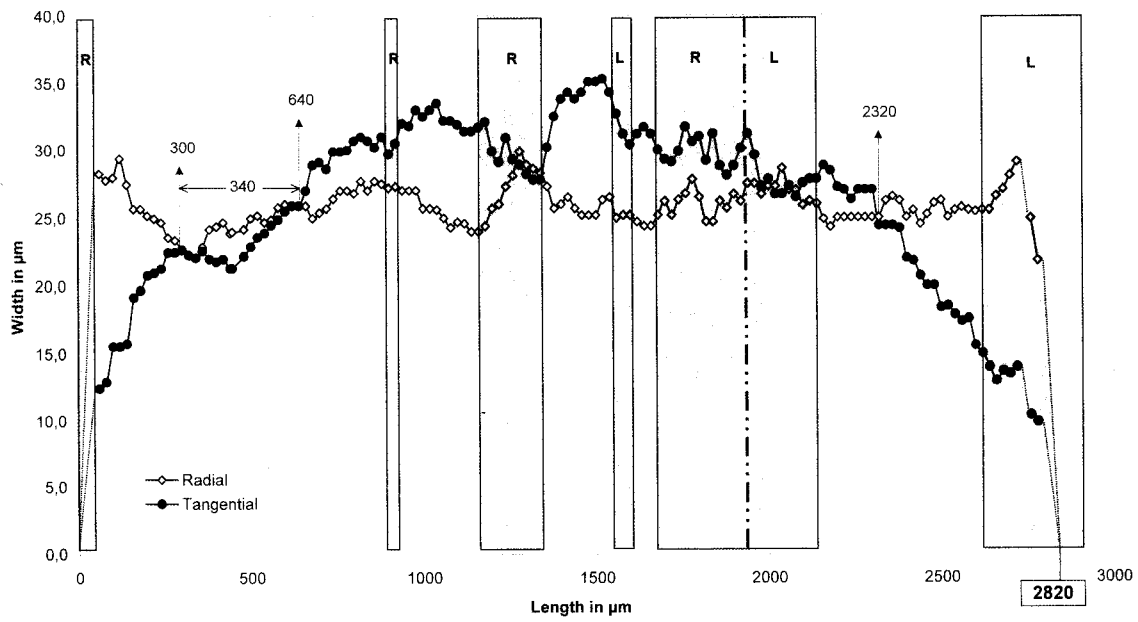


FIG. 3.

Dimensional variation along the length of tracheid 9

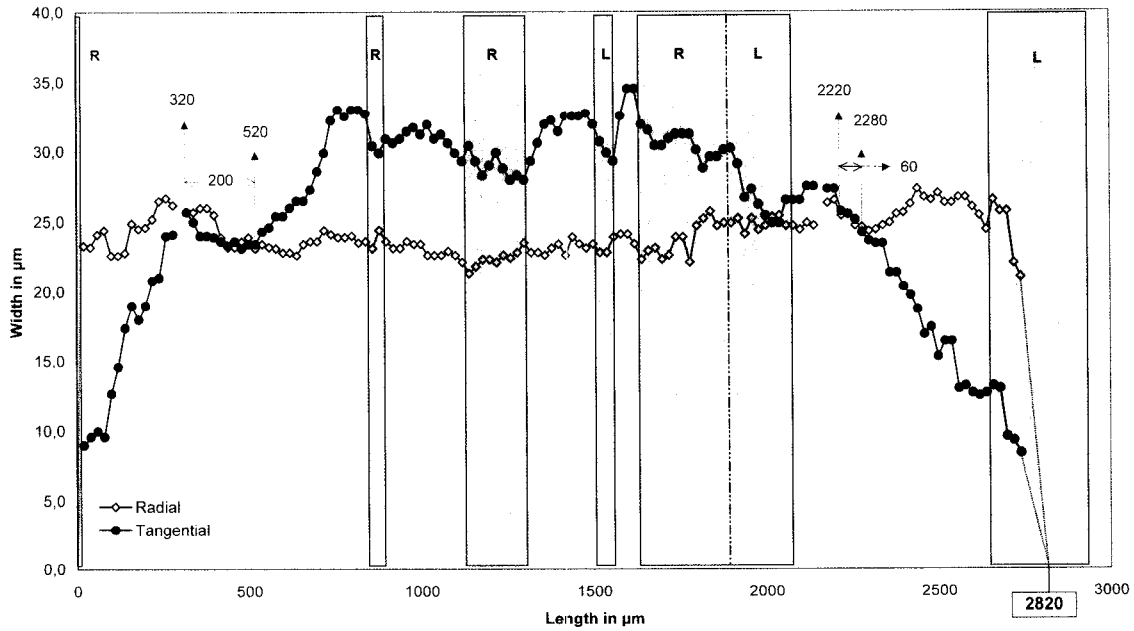


FIG. 4.

TABLE 1. Length of the tracheids studied. The shortest unit length corresponds to 20 μm .

Tracheid no.	Length in μm						(Tip 1/Tip 2)
	Tip 1	T-zone 1	Middle zone	T-zone 2	Tip 2	Total length	
9	320	200	1700	60	540	2820	1.69
8	300	340	1680	20	500	2820	1.66
7	180	340	1940	20	380	2840	2.11
6	200	40	2220	20	380	2840	1.9
Average	250	230	1885	30	450	2830	1.84
ca.	9%	8%	67%	1%	16%	100%	

(version 4.0) and Rhinoceros (version 1.1). Mathematical and statistical calculations were performed with Microsoft Excel 97. The morphological variation within each tracheid transverse section was plotted along the total tracheid length. 3D reconstructions of tracheid segments were generated combining CAD (computer aided design) and visualization softwares. The images were aligned in relation to each other with the help of reference points (year ring border, rays, and neighboring tracheids). The transverse shape of tracheids was extracted from each image and positioned in sequence in the computer. 3D reconstruction was accomplished by separating the serial planes in the Z direction with a corresponding gap of 20 μm in between and linking the serial tracheid segment shapes using Non-Uniform Rational B-Splines (NURBS). Visualization was accomplished with a high degree of freedom, although here they are only displayed in tonalities of the grayscale. Although bordered and cross-field pits are of high importance in the study of tracheid microstructure, they were not displayed in the reconstructions presented in this work. A section thickness of 20 μm was necessary to get a complete set of transverse sections covering whole tracheids. This section thickness did not allow the detailed reconstruction of bordered and cross-field pits. Much thinner sections are needed to allow a more detailed 3D reconstruction of these structures.

RESULTS AND DISCUSSION

Tracheid morphology

Image analysis of serial micrographs revealed that the four latewood tracheids studied

had a characteristic shape with alternating dimensions along the tracheid length. After plotting radial and tangential tracheid width along the tracheid length, it became evident that the tracheids were composed of distinct morphological zones (Figs. 1–4). Five different morphological zones were identified (Fig. 5). The lengths of these different zones are summarized in Table 1. At the beginning of the plots (Figs. 1–4), radial and tangential widths increase progressively, with the radial width exceeding the tangential width until a point where they coincide. This morphological zone was defined as the *first tracheid tip*. The length of this zone varied from 180 μm to 320 μm . Radial and tangential widths remain close with more or less the same value up to a certain length until they begin to delineate. This morphological zone was defined as the *first transition zone*. The length of this zone varied from 40 μm to 340 μm . After delineation, the tangential width increases, stabilizes, and decreases towards a second cross-over, while the radial width remains fairly constant and less than the tangential width. This third morphological zone was defined as the *middle zone*. The length of this zone varied from 1,680 μm to 2,220 μm . At the second cross-over, the radial wall width becomes greater than the tangential width. Here, the change in width dimension occurs more rapidly than at the *first transition zone*. This morphological zone was defined as the *second transition zone*. The length of the *second transition zone* varied from 20 μm (Figs. 1–3) to 60 μm (Fig. 4). Finally, the radial and tangential cell-wall width decreases, with the radial width exceed-

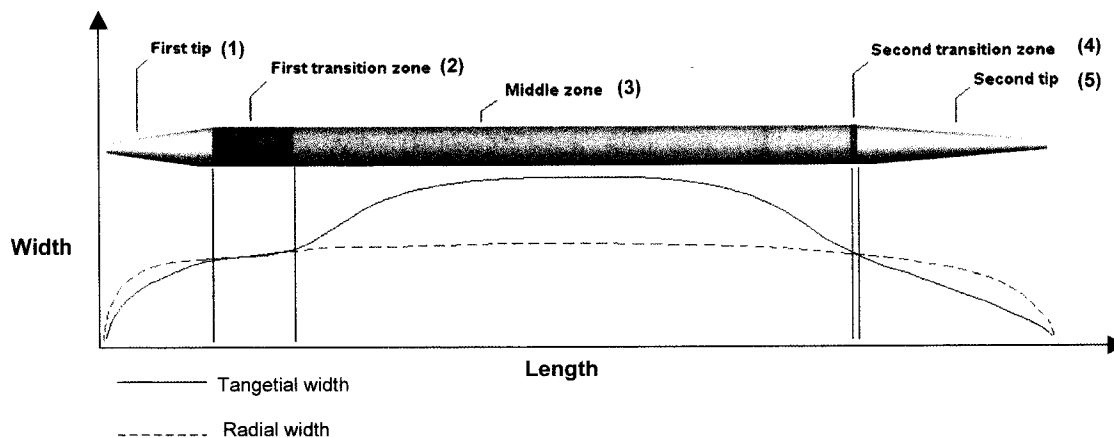


FIG. 5. Schematic representation of the 5 different tracheid morphological zones.

ing the tangential width until they coincide at the very tip of the tracheid. This last morphological zone was defined as the *second tracheid tip*. The length of this zone varied from 380 μm to 540 μm .

A closer examination of the plots revealed other interesting features. The tracheids studied were arranged radially in the same row with tracheid 6 closest to the annual ring border at the latewood side and tracheid 9 the most distant. Taking this into consideration, it is interesting to note that there is a change in dimension that seems to be closely related with the position of the tracheids in the row (Table 1). The length of the tracheid tips and transition zones showed a trend in becoming shorter towards the annual ring border. On the contrary, middle zones seem to become longer. A closer look at the dimensions of tracheid tips and transition zones revealed that the *first tracheid tips* are shorter than the *second tracheid tips*, and that on the contrary the *first transition zones* are larger than the *second*

transition zones (Table 1, Figs. 1–4). This indicates that it should be possible to define the orientation of these tracheids in the stem with one tip pointing upwards and the other downwards. Unfortunately, this was not possible in this study. The data presented in Table 2 also show that the mean width dimensions as well as maximal width dimensions decrease towards the annual ring border. On the contrary, the tangential width at the point of maximal radial width increases towards the annual ring border. This implies that the *middle zone* morphology is also varying along the tracheid row.

Although tracheid width in Norway spruce has not been studied in such detail previously, some comparison with data by Fengel (1969) might be valid. In his work, the mean radial and tangential “diameters” of latewood tracheids are 13.1 and 32.1 μm , respectively. In the present study, the mean radial width of the tracheids studied varied from 17.8 μm to 25.9 μm , and the mean tangential width from 23.6

TABLE 2. Radial and tangential widths along the tracheid length.

Tracheid no.	Radial width (μm)			Tangential width (μm)		
	Mean	Max.	Tang. width at max.	Mean	max.	Rad. width at max.
9	24.1	27.3	18.7	25.4	34.5	24.1
8	25.9	29.9	28.9	26.4	35.3	26.3
7	20.2	24.6	30.3	24.8	32.5	19.2
6	17.8	20.5	31.7	23.6	31.7	20.5

TABLE 3. *Tracheid length comprising cross-field pit regions.*

Tracheid no.	Length in μm								TOTAL	[Right	Left]
	Tip 1		Middle zone		Tip 2						
	Right	Left	Right	Left	Right	Left					
9	20	0	460	280	0	180	940	500	440		
8	60	0	460	280	0	200	1000	540	460		
7	40	0	460	280	0	240	1020	520	500		
6	60	0	460	280	0	240	1040	540	500		
Average	45	0	460	280	0	215	1000	525	475		

μm to 26.3 μm . On the other hand, maximum radial width ranged from 20.5 μm to 29.9 μm and maximum tangential width from 31.7 μm to 35.5 μm . Maximum values were expressed at the *middle zone* of the tracheids, which corresponds on average to ca. 67% of the tracheid length (Table 1). The discrepancy found between these results may not be very relevant because of the limited number of tracheids measured in the present study, but it indicates that measurements made on random transverse sections of wood block may fail to consider the morphological variations along tracheid lengths and tracheid rows. The great variation in data derives from the mean values of all measured transverse and tangential tracheid widths, which undoubtedly are measured at different tracheid lengths. Tracheid measurements may be over- or underestimated, which may have implications on the modeling of wood and wood fiber properties. Modeling of fiber properties may be improved by a better knowledge of the three-dimensional tracheid morphology. The use of 3D modeling techniques to study the morphological variation of tracheids within annual rings, in the same row, and between rows will provide the means to improve modeling of fiber properties.

The plots (Figs. 1–4) also show the occurrence of contact regions with rays or cross-field pit regions and their location along the tracheid length. For ease of understanding, the position of neighboring rays is denoted as **right** and **left** as seen from a tangential point of view. A total of seven rays were in contact with the tracheids studied. At the *first tracheid tips*, there was only one ray passing on the

right, and at the *second tracheid tips* a ray passing on the left. No rays were in contact with the *transition zones*. The highest frequency of contact with rays was at the *middle zones* where three rays were passing on the right and two on the left of the tracheids. A decrease and subsequent increase in tangential widths followed each contact with the rays. Around 1000 μm of the tracheid length was in contact with rays. Approximately 500 μm of contact areas were located on the right side of the tracheids and ca. 500 μm were located on the left side. In average 740 μm of contact areas were located at the *middle zones* (Table 3). This corresponds on average to ca. 40% of the total length of *middle zones*. In these areas the cellulose microfibrils change orientation when passing around the pits in the cell wall (Bailey and Vestal 1937). The orientation of cellulose microfibrils (i.e., microfibril angle) is also believed to affect the mechanical properties of wood fibers (Watson and Dadswell 1964; Page and El-Hosseiny 1983; Cave and Walker 1994).

Cell-wall thickness was also shown to vary along tracheid length (Fig. 6). At the tracheid tips, the average thickness of the tangential wall was greater than the radial wall. *Transition zones* are also reflected in cell-wall thickness. After delineation towards the middle of the tracheid, the thickness of the radial wall becomes greater than that of the tangential wall. Cell-wall thickness varied between ca. 2 μm to 7 μm along the tracheid length (dried state). By performing a linear regression using the average value of cell-wall thickness, it is possible to extract an equation that predicts the

Cell wall thickness along the length of tracheid 8

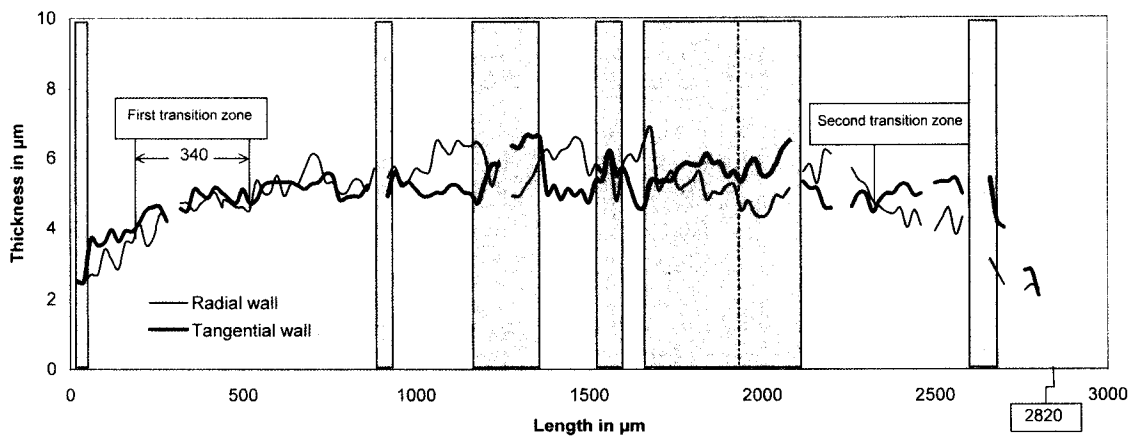


FIG. 6. Variation in radial and tangential cell-wall thickness along the length of Tracheid 8 measured from dried transverse sections. Values are averages between the parallel cell walls in both directions. Shaded areas represent neighboring rays.

average cell-wall thickness along the tracheid length (Fig. 7). The regression curve shows a rapid increase in average cell-wall thickness from the tips of the tracheids towards the middle region, where the average cell-wall thickness increases and decreases progressively at a very low rate. Another possibility is that the data presented here may also reflect the rate of cell-wall deposition in the different segments of the tracheid.

3D reconstruction

Visualization of the gross morphology of tracheids was accomplished using a 3D reconstruction method described in this work. Figure 8 shows in detail 3D reconstructions of three different morphological zones of tracheid 6 in a dry state. Radial and tangential widths vary from the tracheid tip towards the middle. In Fig. 9, segments belonging to the

Average of tangential and radial cell wall thickness along the length of tracheid 8

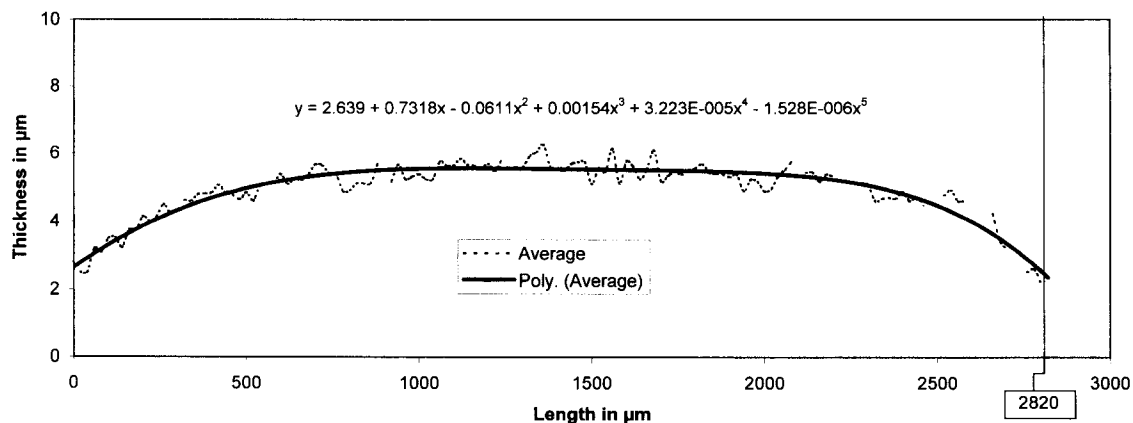


FIG. 7. Variation in average cell-wall thickness along the length of Tracheid 8 measured from dried transverse sections together with a linear regression curve.

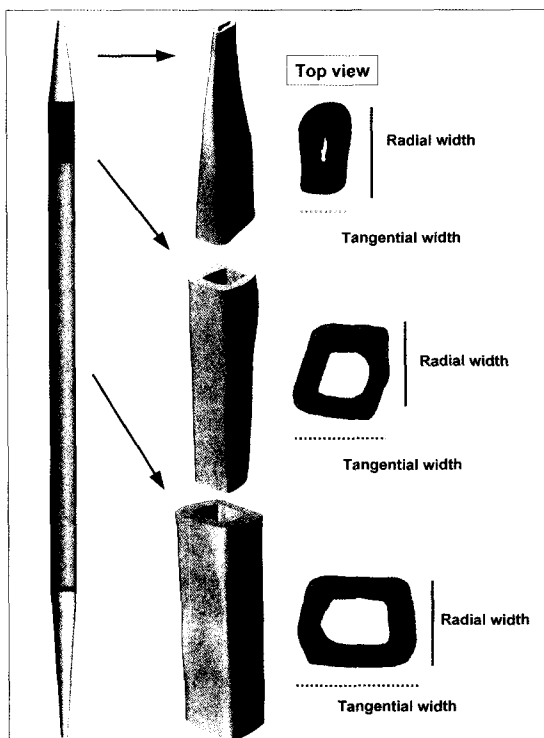


FIG. 8. 3D reconstruction of 100- μm tracheid segments generated from dried transverse sections. The shapes of segments from the *first tracheid tip*, *first transition zone*, and *middle zone* of a tracheid are displayed. Note the change in radial and tangential widths along the length of the tracheid.

different morphological zones of the four tracheids studied are shown. The segments are reconstructed in a row exactly as they were arranged in the wood matrix. Figure 10 displays 14 hydrated latewood tracheid segments distributed in four rows. A new tracheid row is seen emerging on the lower right of the reconstruction where the segments of tracheid tip regions are visualized. In this reconstruction, the possible effect of hydration on the shape of the cell walls is also shown. Tracheid cell walls are seen irregular in thickness and expanded into the tracheid lumens.

Volumetric changes in relation to hydration state of three neighboring latewood tracheid segments were studied with 3D reconstructions (Fig. 11). Three 40- μm -long neighboring tracheid segments were reconstructed. The

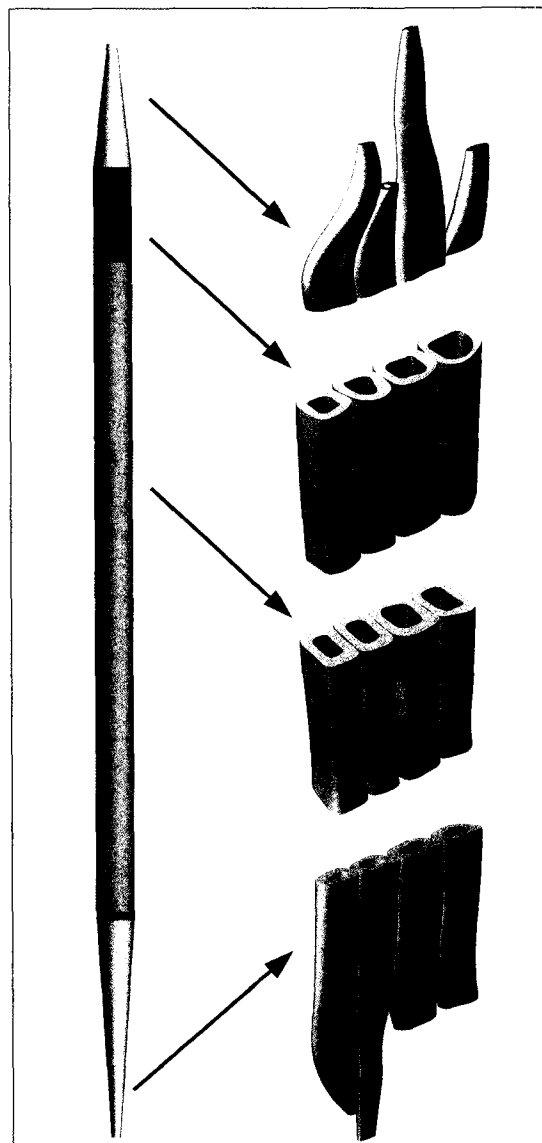


FIG. 9. 3D reconstruction of segments of the tracheids studied showing their position in relation to each other in the wood structure.

samples containing the tracheid segments were first mounted on an objective glass with water. This allowed the acquisition of sequential images of fully hydrated tracheid segments. Thereafter, these same samples were dried prior to observation with a SEM, which allowed the acquisition of sequential images of dried tracheid segments. Two *middle zones* (1 and

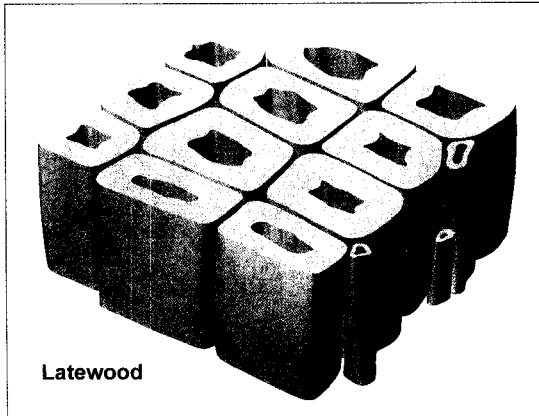


FIG. 10. 3D reconstruction of a segment of latewood tissue showing different fiber segments. This reconstruction was generated from hydrated transverse sections. Note the fiber tips of a new tracheid row appearing on the lower right side of the reconstruction.

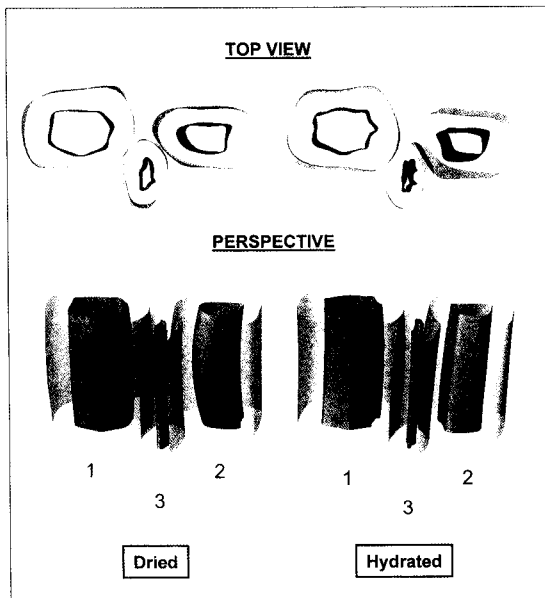


FIG. 11. 3D reconstruction of three neighboring tracheid segments in dried and hydrated states. Reconstructions 1 and 2 are from segments of the middle zone of these tracheids. Reconstruction 3 is from one of the tips of the tracheid. Note the shape of the cell lumen in the different states.

TABLE 4. Measurement of cell wall volume of three 40- μm -long tracheid segments. Segments 1 and 2 are from middle zones of two neighboring tracheids and segment 3 from a neighboring tracheid tip.

Tracheid segments	Dried state (μm^3)	Hydrated state (μm^3)	Volume increase (%)
1	57.66	60.44	4.6
2	39.98	42.28	5.4
3	20.67	20.79	0.6

2) and one tracheid tip (3) are displayed in Fig. 11. Results from measurements of the cell-wall volume (Table 4) revealed that in the presence of water there was ca. 5% increase in total volume of the cell wall of the *middle zones* but only a 0.6% increase of the cell-wall volume at the tracheid tip. As seen in the 3D reconstruction (Fig. 11), the cell walls swell in the presence of water. As a consequence of swelling, the cell walls expand inward towards the lumen (Figs. 11 and 12). Although the shape of the tracheid tip changed slightly after hydration, the cell-wall volume at the tip remained practically the same. This may have occurred because of the limited size of its lumen in combination with a thinner cell wall and by the action of forces applied by expanding neighboring tracheids. Watanabe et al. (1998) described how the cell walls of early-wood tracheids of some coniferous woods

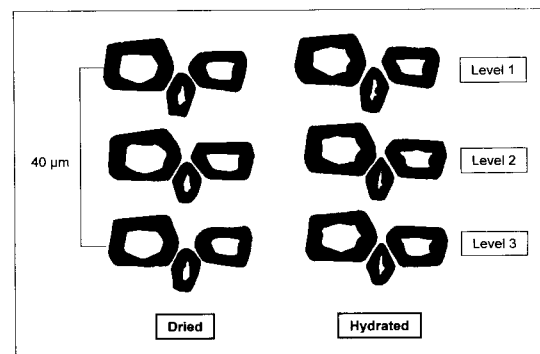


FIG. 12. Transverse shape of the three neighboring tracheid segments in dried and hydrated states at three different planes. The distance between planes in de Z direction is 20 μm . Note the varying distance between tracheids (i.e., varying thickness of the middle lamellae).

shrink after drying, using a replica technique. They also found that normal earlywood of *Cryptomeria obtusa* shrank anisotropically by drying. Radial cell walls shrank less than tangential cell walls, a feature that was almost also constant for the other species they studied. Shrinkage measurements were made on two-dimensional photos showing tracheid transverse sections. In the present work, shrinkage of cell walls was measured as the change in the cell-wall volume of tracheid segments. The swelling of the cell wall of latewood tracheids is more dramatic because of the greater thickness of the cell wall compared with the thickness of the cell wall of earlywood tracheids. The swelling of the cell wall inwards may also build up internal forces that may for instance prevent latewood pulp fibers from collapsing (Jang and Seth 1998). Anisotropic shrinkage of the middle lamellae region between the three neighboring tracheids studied was also observed (Fig. 12). The distance between the tracheids changed depending on the hydration state and level within the 3D wood structure. Although this feature was observed, no attempts to measure dimension changes of the middle lamellae were made in this study.

CONCLUSIONS

The results from this work indicate that there is a potential for the use of computerized 3D reconstruction of wood tissues to improve modeling of wood structure and ultrastructure. The systematic study of whole tracheid morphology will offer the means to develop more accurate models of wood and wood fibers and may improve the modeling of fiber properties. Nevertheless, 3D reconstruction techniques will allow a better interpretation of microscopical sections of wood tissue as well as the physical behavior of wood and wood fibers.

ACKNOWLEDGMENTS

This work was carried out within the framework of the Wood Ultrastructure Research Centre (WURC), a competence center at the

Swedish University of Agricultural Sciences and the SLU Wood Chain Program. WURC was established in cooperation with the Swedish National Board for Industrial and Technical Development (NUTEK), seven companies within or connected with the Swedish forest industry, and four Swedish Universities/research institutions. Part of the SEM observations were performed at the research facilities of AssiDomän Tech Center, Piteå, Sweden, which we gratefully acknowledge.

REFERENCES

- ATMER, B., AND T. THÖRNQVIST 1982. The properties of tracheids in spruce (*Picea abies*) and pine (*Pinus sylvestris*). Department of Forest Products, SLU. Report NR. 134, p. 80.
- BAILEY, I. W., AND M. R. VESTAL 1937. The orientation of cellulose in the secondary wall of tracheary cells. *J. Arnold Arbo.* 18:185–195.
- BANNAN, M. W. 1965. The length, tangential diameter, and length/width ratio of conifer tracheids. *Can. J. Botany* 43:967–984.
- CAVE, I. D., AND J. C. F. WALKER 1994. Stiffness of wood in fast-growing plantation softwoods: The influence of microfibril angle. *Forest Prod. J.* 44(5):43–48.
- EMONS, A. M., AND B. M. MULDER 1998. The making of the architecture of the plant cell wall: How cells exploit geometry. *Proc. Natl. Acad. Sci. USA. Plant Biology* 95:7215–7219.
- FENGEL, D. 1969. The ultrastructure of cellulose from wood. Part 1: Wood as the basic material for the isolation of cellulose. *Wood Sci. Technol.* 3:203–217.
- FUJII, T. 1993. Application of a resin casting method to wood anatomy of some Japanese Fagaceae species. *IAWA-Journal* 14(3):273–288.
- FUJITA, M., AND H. SAIKI 1996. Three-dimensional analysis of vessels in *Aesculus turbinata*. Recent advances in wood anatomy. Pages 45–46 in *Proc. Third Pacific Regional Wood Anatomy Conference*, Rotorua, New Zealand.
- HELANDER, B. A. 1933. Variations in tracheid length of pine and spruce. *Found. Forest Prod. Res. Finland.* 14: 75.
- HERMAN, M., P. DUTILLEUL, AND T. AVELLA-SHAW 1998. Intra-ring and inter-ring variations of tracheid lengths in fast-grown versus slow-grown Norway spruce (*Picea abies*). *IAWA Journal* 19:3–23.
- JANG, H. E., AND R. S. SETH 1998. Using confocal microscopy to characterise the collapse behaviour of fibres. *TAPPL* 81(5):167–173.
- KOLLMANN, F. F. P., AND W. A. CÔTÉ 1984. Principles of wood science and technology. Springer-Verlag, Berlin, Heidelberg, New York, Tokyo.

- LEWIS, F. T. 1935. The shape of the tracheids in the pine. *Am. J. Botany* 22:741-762.
- LINDSTRÖM, H. 1997. Fiber length, tracheid diameter, and latewood percentages in Norway spruce: development from pit outwards. *Wood Fiber Sci.* 29:21-34.
- NAKATO, K., AND S. KAJITA 1955. On the cause of anisotropic shrinkage and swelling of wood (IV). On the relationships between the annual ring and the anisotropic shrinkage. *J. Jop. For. Soc.* 37(1):22-25.
- PAGE, D. H., AND F. EL-HOSSEINY 1983. The mechanical properties of single pulp wood fibres. Part IV. Fibril angle and the shape of stress-strain curve. *J. Pulp Paper Sci.* 84(9):TR99-100.
- PANSHIN, A. J., AND C. DE ZEEUW 1980. The minute structure of coniferous woods. *Textbook of wood technology*, 4th ed, McGraw-Hill, New York, NY P. 772.
- PENTONEY, R. E. 1953. Mechanisms affecting tangential vs. radial shrinkage. *J. Forest Res. Soc.* 3(2):27-32.
- SARÄMPÄÄ, P. 1994. Basic density, longitudinal shrinkage and tracheid length of juvenile wood of *Picea abies* (L.) Karst. *Scand. J. Forest Res.* 9:68-74.
- SUZUKI, K., M. FUJITA, AND H. SAIKI 1991. Three-dimensional reconstruction of wood cell axes by connecting the centers of gravity of cell sections. *Bull. Kyoto Univ. Forestry* 63:246-255.
- TYRVÄINEN, J. 1995. Wood and fiber properties of Norway spruce and its suitability for thermomechanical pulping. *Acta For. Fenn.* 249:155.
- VASILJEVIC, S. 1955. Tracheid length within the growth ring. *Glasn sum Fak, Beograd* 10:161-190.
- WANG, H., AND S. M. SHALER 1998. Computer-simulated three-dimensional microstructure of wood fibre composite materials. *J. Pulp Paper Sci.* 24:314-319.
- WATANABE, U., M. FUJITA, AND M. NORIMOTO 1998. Transverse shrinkage of coniferous wood cells examined using replica method and power spectrum analysis. *Holzforschung* 52:200-206.
- WATSON, A. J., AND H. E. DADSWELL 1964. Influence of fibre morphology on paper properties. *Appita* 17(6): 151-156.
- ZELLING, G., AND A. PERKTOLD 1998. Diurnal stress-related ultrastructural changes in 3D reconstructed chloroplasts. *In* H. A. Calderón Benavides and M. José Yacamán, eds. *Electron microscopy: Advances in microscopy of plant biology, and electron microscopy of natural resources* 4:21.